

1 **Tree height in tropical forest as measured by different ground, proximal, and remote sensing**  
2 **instruments, and impacts on above ground biomass estimates.**

3 **Authors:** Gaia Vaglio Laurin<sup>a,d</sup>, Jianqi Ding<sup>b</sup>, Mathias Disney<sup>c</sup>, Bartholomeus Harm<sup>b</sup>, Martin Herold<sup>b</sup>, Dario  
4 Papale<sup>a</sup>, Riccardo Valentini<sup>a,d</sup>.

5 <sup>a</sup>Department for Innovation in Biological, Agro-Food and Forest Systems (DIBAF), University of Tuscia,  
6 01100 Viterbo, Italy

7 <sup>b</sup>Laboratory of Geoinformation Science and Remote Sensing, Wageningen University, Wageningen, 6708  
8 PB The Netherlands

9 <sup>c</sup>Department of Geography, University College London, Gower Street, London WC1E 6BT, UK

10 <sup>d</sup>Impacts of Agriculture, Forests and Ecosystem Services Division, Euro-Mediterranean Center on Climate  
11 Change (IAFES-CMCC), via Pacinotti 5, Viterbo 01100, Italy

12

13 **Abstract**

14 Tree height is an important structural trait, critical in forest ecology and for above ground biomass estimate,  
15 and difficult to accurately measure in the field especially in dense forests, such as the tropical ones. The  
16 accuracy of height measurements depend on several factors including forest status, the experience of the  
17 observer, and the equipment used, with large subjectivity, heterogeneity and uncertainty in results, that can  
18 propagate when tree height is used in models. A comparison of Terrestrial Laser Scanning, Airborne Lidar  
19 Scanning, and stereo-photogrammetry (with imagery acquired by a RGB camera mounted on Unmanned  
20 Aerial Vehicle) approaches for estimating tree height was here performed, also with reference to ground  
21 methods. In fact, all those technique may increase the possibility of precise tree height measures, while  
22 reducing manual effort in comparison to more traditional ground techniques. The research was carried out in  
23 a dense tropical forest in Ghana; differences in measured heights as well as their impact on above ground  
24 biomass estimation were analyzed. All the different methods were characterized by pros and cons: the  
25 obtained results indicate that in dense forests, where sight occlusion problems occur, ground traditional  
26 techniques can lead to overestimation, while with the other mentioned techniques underestimation can occur,  
27 but in variable amount according to the considered instrument. The different height measures caused a  
28 remarkable variation in the estimated biomass of this tropical forest: more accurate height measurements are  
29 needed to reduce the uncertainty in biomass mapping efforts at any scale. Possibly, the simultaneous use of  
30 different methods can help in correctly estimate height uncertainty and reach a convergent and accurate  
31 result.

32

33

34 **Keywords:** tree height; forests; biomass; UAV lidar; ALS, photogrammetry; TLS

35

36

37

38 The authors have no competing interests to declare.

39

40

41

42

43

44

45

46

47

## 48 1. Introduction

49 Tree height is an important ecological trait, and part of many natural resource data collections, being the  
50 most widely used indicator of a site's fertility and suitability for a variety of stand management uses, ranging  
51 from wildlife habitat to timber production. Tree height can also provide indications on forest health  
52 conditions, as climate-induced events can alter growth processes, and disturbance can impact the height of  
53 selected individuals and stands. Tree heights are often measured in ecological and biodiversity studies or  
54 modeled to characterize life histories of species and populations (Banin et al. 2012, Kruger et al. 1997). In  
55 computing above ground biomass (AGB) this information is crucial, with previous work demonstrating that  
56 the incorporation of height into allometric models in addition to the diameter variable significantly improves  
57 AGB estimates, especially in tropical forests (Feldpaush et al. 2012). At present, most of the widely adopted  
58 models include the height variable.

59 Tree heights can be however difficult to accurately measure in the field, especially in tropical forests where  
60 tall, closed canopies, and dense understory occur, limiting the sight of tree tops (Rennie 1979). The accuracy  
61 of height measurements thus depend on forest conditions, but also on the experience of the observer, and the  
62 equipment used, leading to a large subjectivity and heterogeneity. In the ground, the various methods  
63 adopted to measure individual tree height can produce different results, as illustrated by Larjavaara and  
64 Muller-Landau (2013) who compared the sine and the tangent methods. Hunter et al. (2013) identified five  
65 sources of uncertainty that contribute to the precision of tropical field height measurements, including the  
66 offset between measured distance and crown-top position, tree-top occlusion, ground slope, obstacles for  
67 distance measurements, and clinometer operator error.

68 Even when using the same technique, differences in the way the instrument is set or the data are acquired can  
69 impact the results. Yu et al. (2004) in a lidar-based study showed that differences in airplane flight altitude  
70 produced variations in the tree heights estimated from the lidar point clouds. When height is used as input to  
71 calculate AGB, inaccuracy in measures can lead to large errors in biomass estimates (Molto et al. 2013).

72 Also large scale AGB maps derived using remote sensing or models are calibrated and validated using on  
73 site level biomass data, computed through allometric models based on diameters and heights (Avitabile et al.  
74 2016, Saatchi et al. 2001).

75 Among the different techniques that can be used to measure tree heights, here the focus is on Terrestrial  
76 Laser Scanning (TLS), Airborne Lidar Scanning (ALS), and stereo-photogrammetry with imagery acquired  
77 by a RGB camera mounted on Unmanned Aerial Vehicle (UAV). All these approaches increase the  
78 possibility of precise tree height measures while reducing manual effort in comparison to more traditional  
79 techniques, such as manual laser distance meter or clinometer.

80 TLS is a laser-based instrument used in the field to acquire precise range and angular measurements by  
81 means of the optical beam deflection mechanism. From TLS, a 3D point cloud of the scanned volume is  
82 obtained, and information on forest structure, including trees diameter and height, can be derived (Liang et  
83 al. 2016). The highest point over the ground close to the tree stem is collected, and then the value of the  
84 corresponding highest cloud point is considered as the tree height. TLS allows to scan a forest stand faster  
85 than traditional methods, and its use in forest resource surveys has recently increased (Srinivasan et al.  
86 2015). However, similarly to other field-based techniques, due to occlusion problems the heights extracted  
87 from TLS point cloud can result lower than the actual values (Brede et al. 2017, Liu et al. 2016).

88 With ALS the distance from the sensor on an airplane to a target can be measured through pulsed laser light:  
89 the differences in laser returns time can then be used to make a digital 3-D representation of the target thanks  
90 to the laser penetration capability (Rosca et al., 2018). In ALS surveys covering forests, the point cloud is  
91 classified and interpolated to obtain a Digital Surface Model and a Digital Elevation Model, and by  
92 subtraction a Canopy Height Model (CHM) which contains the real height from the ground. The CHM is  
93 then filtered, usually with local maxima algorithms, to identify single trees metrics. With airborne surveys,  
94 the detection of top canopy is not affected by occlusion issues, but the capability to precisely hit the tree tops  
95 and map the ground level is influenced by various factors, including forest structure, lidar pulse density, scan  
96 angle, platform altitude, and beam size, among others. Different studies reported underestimation of tree  
97 heights with ALS, especially in old growth forests (Andersen et al. 2006, Clark et al. 2004, Goodwin et al.  
98 2006). While many countries already conducted large lidar surveys covering forested areas, ALS data are  
99 unfortunately still not always open access, and surveys are in general expensive.

100 Low cost UAVs systems equipped with a consumer-grade RGB camera can acquire stereo imagery, from  
101 which a high resolution point cloud can be generated and processed to obtain a DSM. Using a local maxima  
102 algorithm the identification of tree tops is possible, and then by means of ground level subtraction, tree

103 heights can be estimated. However, interpolating the terrain with only the few points obtained by stereo  
104 optical imagery, which differently from lidar does not penetrate the canopy, can be a problem (Wallace et al.  
105 2014, Rosca et al., 2018). A high resolution Digital Elevation Model (DEM) obtained from other sources is  
106 therefore necessary to estimate individual tree level metrics. When ground information is available or the  
107 forest terrain is flat, UAVs can represent a cost-effective approach.

108 Only limited information is available on the accuracy of tree heights as measured by different techniques or  
109 sensors over the same forest (Fowler and Kadatskiy 2011, Rosca et al., 2018), in particular in tropical forests.  
110 Considering the high economic costs of forest surveys, independently by the adopted instrument or  
111 technique, a comparative analysis over a single site can be useful, as it provides valuable information to help  
112 decision making in forest resources management and planning. The objective of this research is to  
113 comparatively analyze tree numbers and tree heights as derived by: i) a ground-based traditional technique,  
114 ii) a TLS system, iii) a set of stereo-photogrammetry with imagery from a UAV, and iv) an ALS acquisition.  
115 Specifically, for tree number estimation the ground data were considered as the reference. For tree height, we  
116 present a comparison of different techniques, evaluating their agreement, due to the uncertainty reported  
117 when using ground-based techniques (Hunter et al. 2013; Larjavaara and Muller-Landau 2013; Ronnie,  
118 1979). The impact of different height estimates on the computation of above ground biomass estimation  
119 using allometric equation was also analyzed. The research was realized in a dense tropical forest in Ghana, in  
120 the Ankasa Conservation Area, where occlusion problems are highly relevant.

121

122

## 123 2. Materials and methods

124

### 125 2.1 Study area

126 The study site (Fig.1) is the Ankasa Conservation Area located in southwestern Ghana and composed by the  
127 Ankasa Game Reserve and the Nin-Suhien National Park. Ankasa extends over approximately 509 km<sup>2</sup>:  
128 protected since 1976, it includes a National Park and a Resource Reserve, and represents a remnant spot of  
129 the Upper Guinean forest belt, that once covered all the west African coasts. The area has gentle topography,  
130 with low hills (90 m average elevation) and presence of small swamps, a mean temperature ranging from  
131 24°C to 28°C, high humidity all year round, and average annual rainfall in the 2000-2200 mm range. The  
132 vegetation is wet and moist evergreen forest, with very high floristic and structural diversity, that provides  
133 protection to rare wildlife, including forest elephants, chimpanzees, and leopards. Species typical of this  
134 forest area include: *Cynometra ananta* Hutch. & Dalz., *Lophira alata* Banks ex C.F.Gaertn., *Heritiera utilis*  
135 Sprague, and *Protomegabaria stapfiana* Beille (Hall & Swaine 1981; Vaglio Laurin et al. 2016a, 2016b).  
136 Prior to 1976, in Ankasa borders some logging activities were carried out, and illegal forest disturbance can  
137 still occur (Damnyag et al. 2013). The data collection was realized in the core of the conservation area, in a  
138 0.7 ha research plot of lowland mature moist forest far from past or present disturbance.

139



140

141 Figure 1. The Ankasa Conservation Area (in red) located at the Ghana – Ivory Coast border.  
142  
143

## 144 2.2 Datasets

145 Terrestrial Laser Scanning (TLS) data were collected in March 2016 (dry season) using two Riegl VZ-400  
146 instruments, operating at a wavelength of 1550 nm. Horizontally, the instrument can scan 360° in azimuth  
147 direction and vertically it has a field of view of 100°: 70° above, and 30° below the horizontal plane. 88 scan  
148 positions were set up, in correspondence of the grid nodes resulting from the division of the 0.7 ha plot in 70  
149 10x10 m subplots; 6 reflectors were placed for co-registration purposes in each scan position. 176 TLS point  
150 clouds were collected, and then merged and co-registered using Riegl RiscanPro (Riegl). The accuracy of the  
151 final point cloud was < 1 cm; the dataset was divided into 20 tiles to facilitate data handle; the plot  
152 boundaries as scanned by TLS were used to subset airborne lidar and photogrammetric data.

153 Photogrammetric data were also collected in March 2016 using a Phantom 3 Professional UAV equipped  
154 with a 4K camera. The Pix4Dcapture software (Pix4D) guided the flight plan: 215 RGB images were  
155 collected at 5 cm spatial resolution. Using Agisoft Photoscan Professional software (Agisoft LLC) a point  
156 cloud and orthophotos were produced.

157 Airborne lidar (ALS) data were collected in March 2012 with a Optech GEMINI sensor, having a 1064 nm  
158 wavelength laser, emitting at 167 kHz max pulse repetition frequency and with 0.25-mrad (1/e) beam  
159 divergence, collecting up to 4 range measurements. Mean laser point density ranged between 12 and 20  
160 points per square meter; maximum scan angle of the laser beam was < 11°; positional errors in horizontal  
161 and vertical dimensions were < 0.27 m. The point cloud was classified using Terrascan software (Terrasolid)  
162 into ground and vegetation returns.

163 A botanical survey was realized in March 2016 collecting species, diameter at breast height (DBH), and  
164 height information for trees having DBH above or equal to 10 cm. The height of the trees was measured with  
165 a transponder and vertex meter. Wood density values at species level were extracted from the Global Wood  
166 Density Database (Dryad; Chave et al. 2009); for species not present in the database the genus or family  
167 value was adopted. Above ground biomass (AGB) was computed according to Chave et al. (2014) equation.  
168

## 169 2.3 Data analysis

170 The data analysis workflow included different steps. First, the three point clouds derived by ALS, TLS, and  
171 photogrammetric surveys were co-registered. Three canopy height models (CHM) were then derived from  
172 each of the co-registered point clouds, using the lidar-derived DEM for ALS and the photogrammetry  
173 dataset, and TLS-derived DEM for the TLS datasets. The visible crowns were delineated in the CHMs,  
174 extracting tree-level information using an inverted watershed procedure, and thus deriving heights.

175 A stem map was produced using the fine scale TLS point cloud, manually detecting DBHs of larger trees and  
176 corresponding heights. A univocal match between ground data and selected trees in the stem map was then  
177 established, according to correspondence in positional, DBH and height values. For these selected trees,  
178 height values as measured with different instruments were compared. Above ground biomass was also  
179 calculated using as input into the allometric equation the DBHs from ground database and the heights as  
180 measured by different instruments, to evaluate the impact in carbon stocks estimates at tree and plot level.  
181 All the steps were realized using CloudCompare and ArcGIS software.  
182

### 183 2.3.1 Point clouds co-registration

184 A manual exclusion of few outliers found in each dataset was initially performed (Fig. 2). The ALS point  
185 cloud (LPC) was set as the reference dataset for co-registration purposes. The photogrammetric point cloud  
186 (PPC) was firstly co-registered to the ALS one, and then the process was repeated for the TLS point cloud  
187 (TPC).  
188



189  
190  
191

Figure 2. Detection and exclusion of outliers (red circles) from the PPC dataset over the plot.

192 To co-register LPC and PPC, a mesh model was used to convert the points from PPC, having lower density  
193 with respect to LPC, into a surface made by triangular (or quadrilateral) contiguous and non-overlapping  
194 faces joined along their edges. The vertical displacement observed between the LPC and PPC was manually  
195 reduced, using the matching bounding box centers procedure. These initial two steps helped in the  
196 identification of control points. An horizontal and vertical coarse alignment was conducted using four crown  
197 tops pairs as ground control points, clearly detected in LPC and PPC for being very tall trees with  
198 characteristic crown shapes, and evident tree tops that facilitate the vertical alignment. Fine alignment  
199 followed, based on the iterative closest point (ICP) algorithm, which iteratively minimizes the mean square  
200 error between points in a point set and the closest points in the other one (Chen and Medioni 1992; Besl and  
201 McKay 1992); iterations number was set to 20.

202 The co-registration of the LPC and TPC started with a data resampling: the TPC reached 20.6 gigabytes in  
203 size, organized in 20 tiles. To handle such a large dataset the procedure suggested by Theiler (2014) was  
204 followed, subsampling each TPC tile to obtain points spaced by a distance equal to 0.1 m, thus reducing the  
205 data to a sparser set before seeking for correspondent features in LPC. The 20 tiles were merged in one  
206 dataset and four crown tops were identified in TPC and LPC, again selecting tall trees with characteristic  
207 shape. The point clouds for these crowns were extracted from both TPC and LPC, also repeating the co-  
208 registration procedure at finer crown scale. The transformation matrices were recorded and then applied to  
209 the full TPC.

210 To evaluate the alignment result, the cloud to cloud distance was calculated: for each point in the source  
211 cloud, a 'nearest neighbor' is searched in the reference one computing the Euclidean distance.

212

### 213 2.3.2 Canopy Height Model generation

214 Three DSMs were generated from LPC, TPC and PPC. For the classified LPC (ground and vegetation  
215 points), only first returns were converted into a raster using a 'local maxima' interpolation procedure, thus  
216 using the points of maximum height as raster pixel values. For TPC, and PPC the whole point clouds were  
217 used to generate the DSMs.

218 Two DTMs were also generated. For LPC, the interpolation procedure was based on ground returns only and  
219 the selection of 'local minimum'; for TPC, given the high density of points at ground level, no interpolation  
220 procedure was applied, and the minimum value of point height in each pixel was selected as pixel value in  
221 the raster.

222 CHMs, representing the difference between the top canopy surface and the underlying ground topography,  
223 were obtained subtracting the digital terrain model (DTM) from the digital surface model (DSM), both  
224 available from LPC and TPC. From PPC, given the lack of penetration capability, only the DSM was  
225 computed and for CHM generation the DTM derived from LPC was used.

226 To test impact of spatial resolution on tree detection capabilities in tree top detection and for crown  
227 delineation, all the layers were generated at 1m and 0.5m spatial resolution.

228

### 229 2.3.3 Tree crown segmentation crown delineation

230 The variable window filter algorithm (Popescu & Wynne, 2004), as implemented in the ForestTools R  
231 package (Plowright, 2018), was used to detect tree tops from the canopy height models. For the 1m CHM's  
232 the variable window size was determined using a linear function with  $a=0.05$  and  $b=0.6$ , while for the 0.5m  
233 CHM's  $a=0.05$  and  $b=0.5$  were used. Those values were empirically determined for the specific datasets, by

234 systematically increasing both the a and b values with steps of 0.01 and 0.01 respectively. First the b  
235 parameter was optimized, where the plot of detected number of trees for each b-value shows a clear jump at  
236 the ideal b value. Using this b-value the optimal value for a was determined. Again, the value was selected  
237 where number of detected trees plotted against the a-values showed consistent outputs. This was cross-  
238 checked against the number of emergent trees as described in the field-survey.

239 Next the watershed function (Meyer & Beucher,1990) was applied to segment crowns from the canopy  
240 height model, where the segmentation is guided by the point locations of the individual tree tops. For the  
241 individually detected trees summary statistics of the crown dimensions and tree height were calculated.

242

#### 243 *2.3.4 Stem map and DBH from TLS data*

244 To create a stem map, the TPC was segmented at 1.3 m above the ground. Next, a height ramp color was  
245 applied, which made it possible to distinguish the stems from surrounding lower vegetation. The stem map  
246 thus obtained showed several circular or semi-circular shapes corresponding to the tree stems: each stem was  
247 manually segmented. To calculate DBH longest and shortest axis were averaged. For large trees with buttress  
248 structure, the cross section was gradually moved upward until it was regular in shape and the DBH could be  
249 determined. For tilted trees or those growing on slopes, the DBH was measured along the stem direction. To  
250 find the height of trees for which DBH was measured, the stem map was converted into a raster and  
251 superimposed on the CHM. The maximum pixel value around the stem was manually identified also  
252 considering slope direction, and considered as the tree top with correspondent height.

253

#### 254 *2.3.5 Matching trees from remote and ground databases*

255 TLS and botanical ground survey were conducted collecting tree information at subplot level. The stem map  
256 was firstly overlapped to the georeferenced ground data grid. A mismatch between datasets (due to the  
257 imprecise geolocation often occurring under dense forest coverage) was observed, as corresponding subplots  
258 in TLS and ground survey did not include same DBHs and height values. Therefore, a manual search of  
259 corresponding trees in the two dataset was performed: for trees having DBH > 30 cm in the ground database,  
260 the correspondence with a tree in the same subplot or in the surrounding ones was searched in the stem map  
261 and in PPC, allowing a maximum difference of 10% in DBH. Only unequivocally identified pairs were  
262 considered as matched trees. The previous co-registration of all point clouds allowed to establish a match for  
263 those selected trees among the different datasets. Analysis of Variance (ANOVA) was used to determine if  
264 the height of the selected trees, estimated using the different acquisition methods, was significantly different.

265

#### 266 *2.3.6 Above ground biomass estimate*

267 For the selected trees, above ground biomass (AGB) was estimated using the equation from Chave et al.  
268 (2005, 2014); the equation has DBH, wood density, and height as inputs. For DBH, ground collected values  
269 were always used as input in the equation; for height, measures from the different datasets were used.

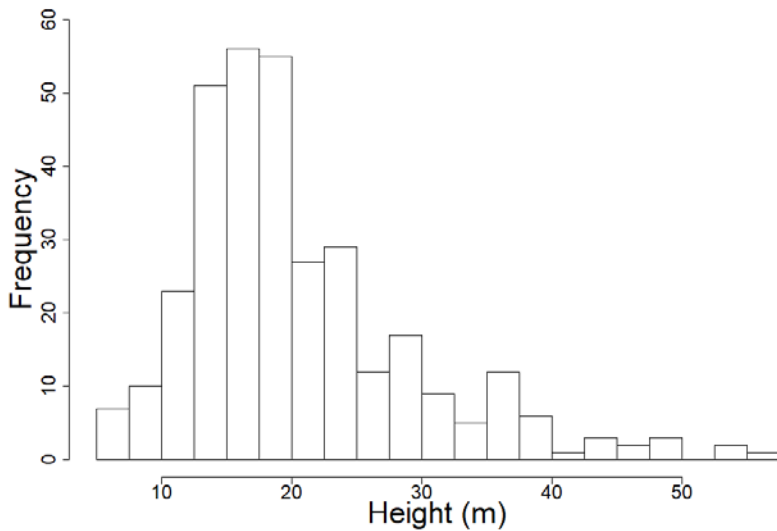
270

271

### 272 **3. Results**

273 A total of 331 trees belonging to 82 different species with DBH > 10 cm were recorded in the botanical  
274 survey; Fig. 3 shows the histogram of height obtained from ground survey, with a recorded maximum height  
275 of 55.5 m and a mean height equal to 20.6 m. The TLS survey recorded 188 trees with DBH > 20 cm.

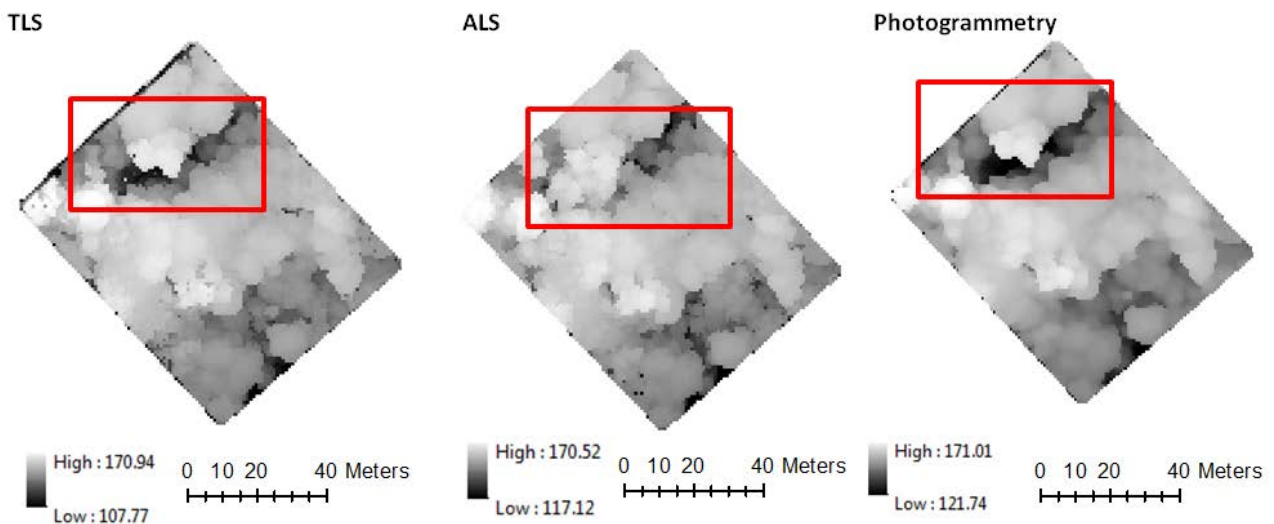
276



277  
278 Figure 3. Distribution of tree heights from ground survey in the 0.7 ha field plot.  
279

280 In the horizontal dimension, the co-registration between LPC and PPC was characterized by a mean point  
281 distance of 0.44 m, a standard deviation equal to 0.52 m, and root mean squared error (RMSE) of 0.62 m.  
282 The co-registration between LPC and TPC showed a mean distance of 0.45 m, a standard deviation of 0.62  
283 m, and an RMSE equal to 0.33 m. In the vertical dimension the cloud to cloud comparison values resulted in  
284 mean differences of only several centimeters (Table 1).

285 The TLS and photogrammetry surveys were both realized in 2016,; the derived DSMs show similar features.  
286 Instead, ALS survey was done in 2012, and the four-year difference in time with respect to other datasets has  
287 to be taken into account. In fact, the ALS-derived DSM shows differences, like the one evidenced in red  
288 rectangle area in Fig. 4, due to changes occurred in the canopy along time.  
289

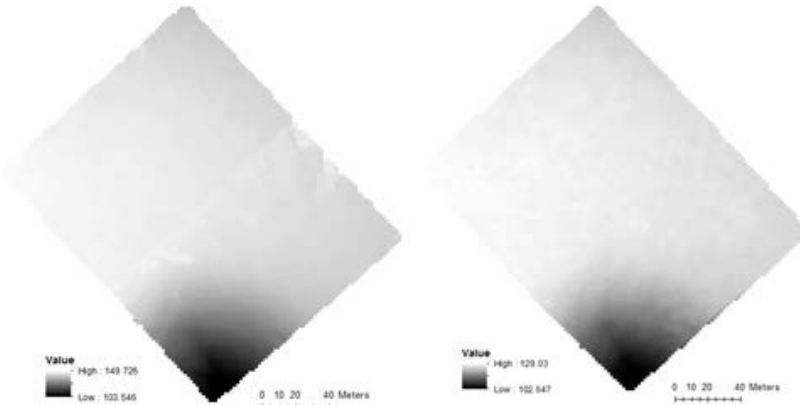


290  
291 Figure 4. DSMs retrieved from TLS, ALS and Stereo Photogrammetry datasets at 1m spatial resolution  
292

293 Table 1: statistics of cloud to cloud distances in the z direction  
294

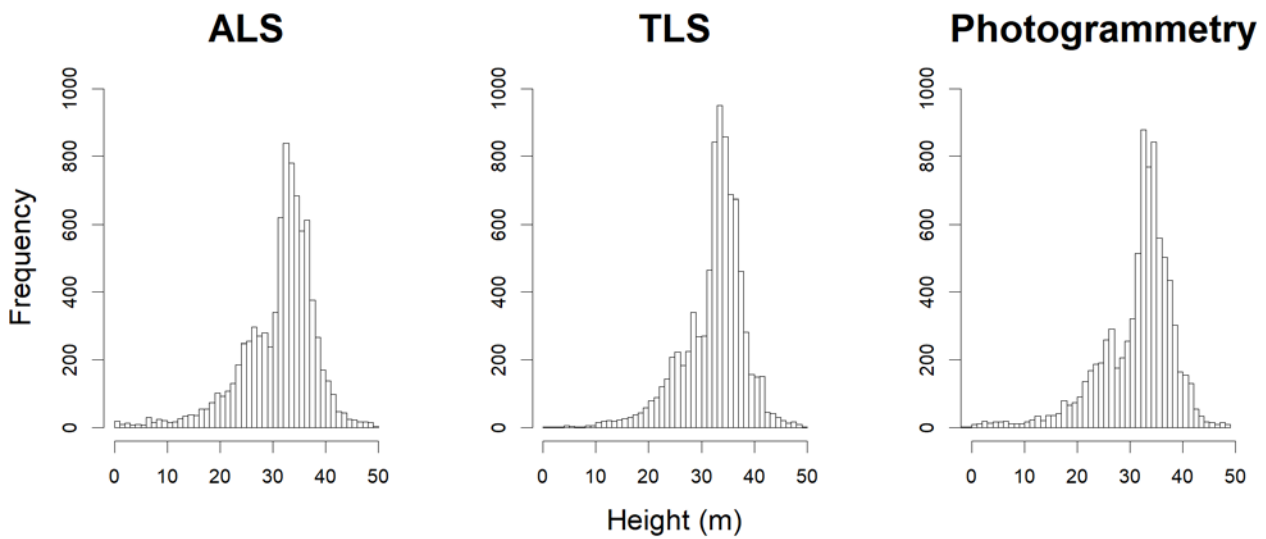
Cloud to cloud	Mean(m)	Std. dev(m)	Min(m)	Max(m)
TLS to ALS	0.09	0.66	-4.03	3.82
PPC to ALS	-0.02	0.49	-3.48	3.67
PPC to TLS	0.00	0.34	-3.74	2.91

300 The two DTM derived from TLS and ALS showed similar features (Fig. 5), with a flat ground and a  
 301 downward slope toward the southeastern corner. The DTM generated with TPC without interpolating ground  
 302 points resulted less smooth with respect to the LPC one.  
 303



304  
 305 Figure 5. DTMs retrieved from ALS (left) and TLS (right) datasets at 1m spatial resolution  
 306

307 The histograms of the three CHMs illustrate the distribution of canopy height model values (Fig. 6). Two  
 308 peaks are visible; the first peak at approximately 33 m for ALS CHM, and at 32 m for TLS and  
 309 photogrammetry CHMs; the second peak is approximately at 28 m, 26 m and 25 m for ALS, TLS and  
 310 photogrammetry data, respectively.  
 311



312  
 313 Figure 6. Histograms for CHMs from TLS, ALS, and photogrammetry, at 1m spatial resolution.  
 314

315 Table 2. Statistics for CHM derived tree segmentations at 1m and 0.5m spatial resolution derived from TLS,  
 316 ALS, and photogrammetry.

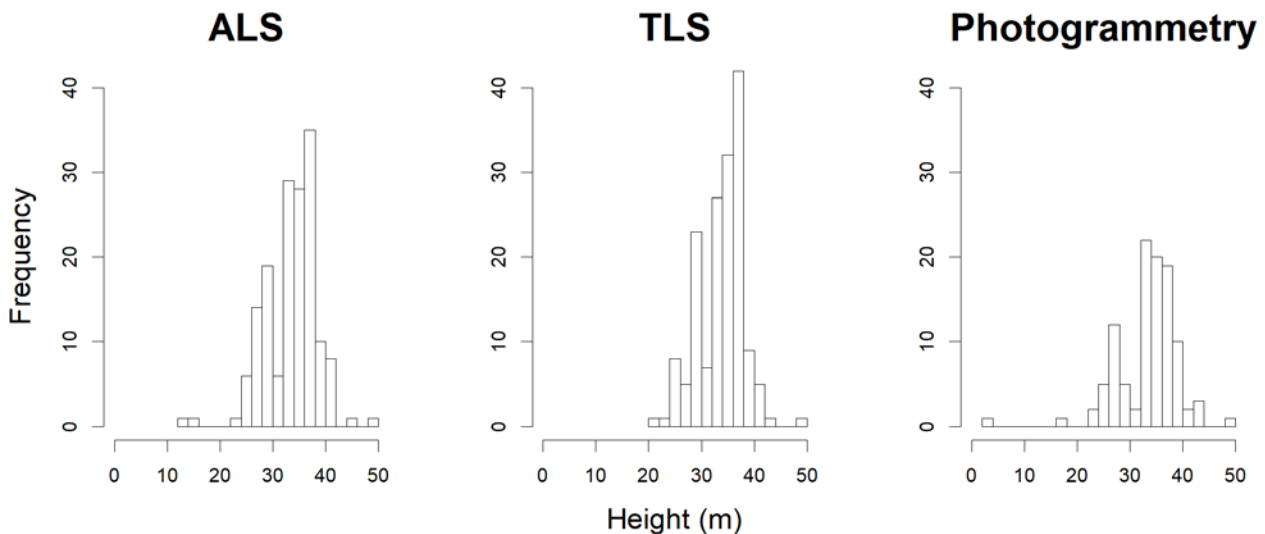
	ALS 1m	ALS 0.5m	TLS 1m	TLS 0.5m	PPC 1m	PPC 0.5m
a	0.05	0.05	0.05	0.05	0.05	0.05
b	0.6	0.5	0.6	0.5	0.6	0.5
Trees	162	160	160	159	105	106
Mean crown area (m <sup>2</sup> )	51.01	51.39	52.01	51.50	78.25	77.31
Median crown area (m <sup>2</sup> )	39	33.5	37	33.5	63	53.38
SD crown area (m <sup>2</sup> )	54.90	54.19	46.31	55.94	59.49	68.53
Min crown area (m <sup>2</sup> )	5	1.5	8	4.5	10	2.25
Max crown area (m <sup>2</sup> )	469	427	288	423.25	328	342



Mean height (m)	33.84	32.25	33.56	32.50	33.39	32.47
Median height (m)	34.57	33.88	34.13	33.63	34.27	33.81
SD height (sd)	4.33	6.65	4.98	6.02	5.82	6.60
Min height (m)	21.02	4.05	13.22	2.76	3.27	2.46
Max height (m)	49.22	49.10	49.27	49.46	48.74	48.22

317  
318  
319  
320  
321  
322  
323  
324  
325  
326  
327  
328  
329  
330  
331  
332  
333  
334

As a result from tree crown segmentation 105 crowns were detected from the photogrammetry CHM, 162 from ALS CHM, and 160 from TLS CHM at 1m spatial resolution, with mean heights equal to 32.47, 33.56 and 33.84 m, respectively. Photogrammetry provided a smoother point cloud for the canopy top and consequently a smoother CHM, thus resulting in a lower number of detected trees. The number of detected trees with ALS and TLS is close to the number of >20cm DBH trees in the inventory. It has to be noted that the number of segmented tree crowns is highly dependent on the a and b parameters in the function fitting. Those values were optimized visually on the TLS datasets and then applied to the other datasets. For the 0.5m CHMs the b parameter had to be diminished, otherwise the number of estimated crowns would have been much higher. It is worth to stress that the optimal a and b values depend on the used datasets and resolution, and the values empirically found may not be directly transferable to other conditions. Table 2 reports the statistics for CHMs derived height and crown size values (0.5m and 1m spatial resolution). The histograms of heights for the tree groups derived from segmentation show considerable differences in height classes distribution (Fig. 7). Furthermore, large differences are found with respect to ground data (Fig. 3); in the ground survey the small trees are included, while with TLS or remote techniques only larger trees are sampled.

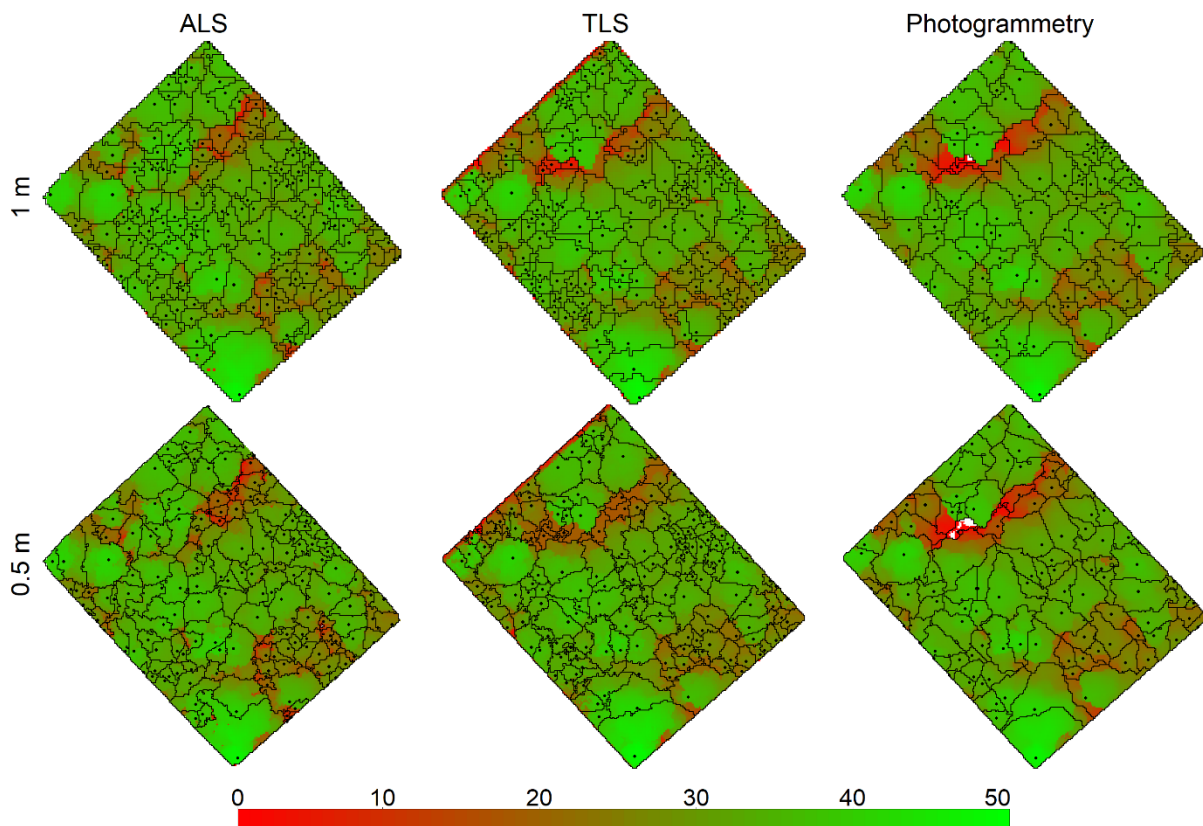


335  
336  
337  
338  
339  
340  
341  
342  
343  
344  
345  
346  
347  
348

Figure 7. Histograms of height detected from ALS, TLS and photogrammetry tree segmentation based on CHMs at 1m spatial resolution.

The detection of crowns resulted in a lower number of tree crowns from the photogrammetry CHM, which obviously influences the statistics about the crown dimensions.

Fig. 8 shows the individual crowns delineation at the two spatial resolutions for the different acquisition techniques. Although differences are clearly visible, the mean crown size for ALS and TLS are comparable, even for the different CHM resolution when the segmentation parameters are adapted. With photogrammetry the lower number of detected tree tops also results in larger crown segments. The spatial distribution of areas with larger or smaller tree crowns is the same for all three acquisition techniques, but both LiDAR techniques distinguish much more smaller trees than photogrammetry does.



350

351

352

353

354

355

356

357

358

359

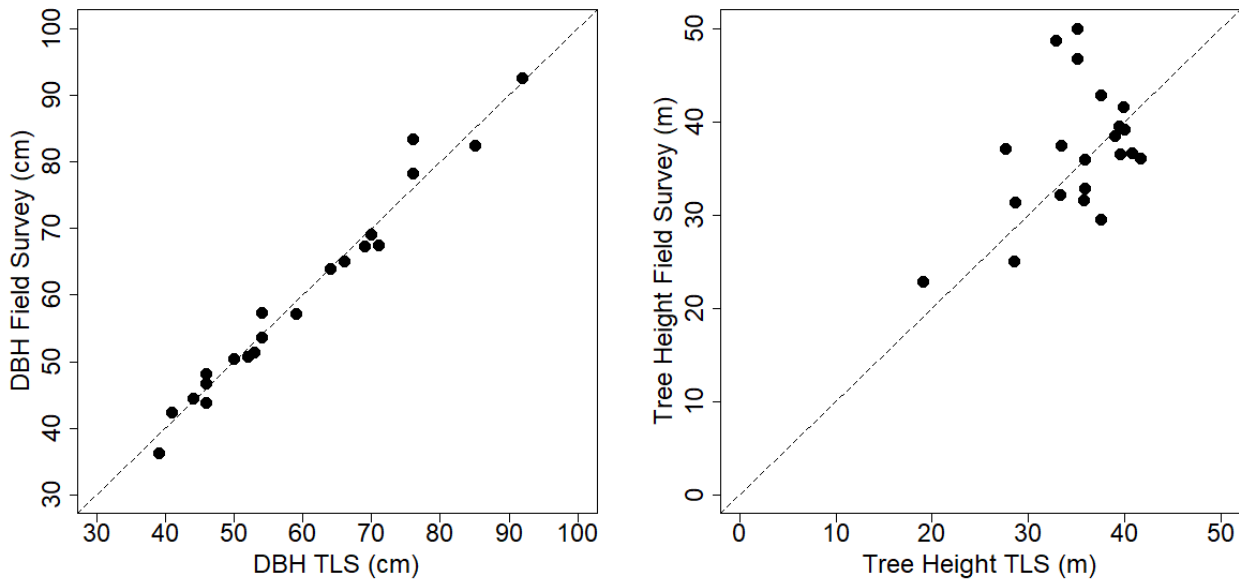
360

361

362

Figure 8. Tree detected using tree crown segmentation at 1 m (top) and 0.5m (bottom) spatial resolution for the ALS, TLS, and photogrammetry datasets.

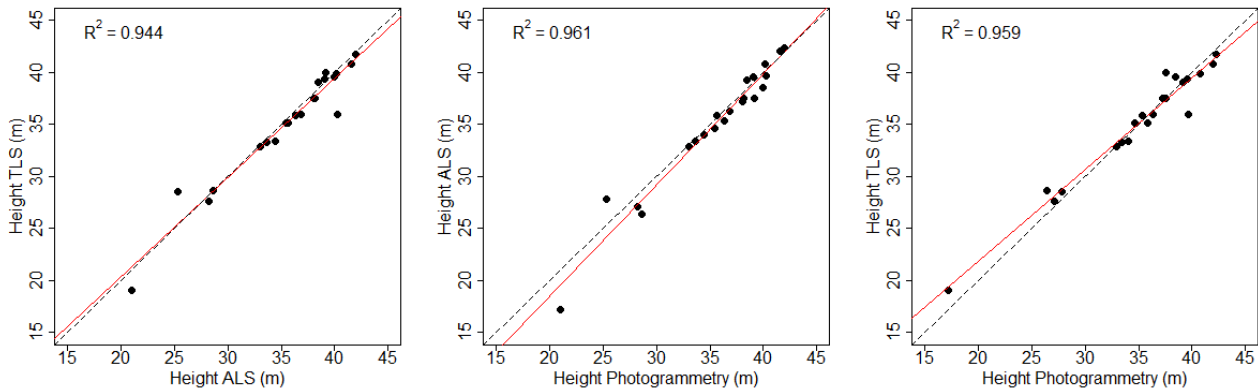
From the stem map derived from TLS data, 38 trees with  $DBH > 30$  cm were clearly detected. However, only 21 tree pairs were univocally identified in ground and TLS databases. The average height of these trees as from TLS data resulted equal to 35.3 m, while from ground data to 37.2 m, almost 2 m higher than the previous. The ANOVA results show that there is no statistically significant difference between the mean heights derived with the different techniques (F-value = 0.367). The RMSE for DBH values resulted equal to 2.38 cm, while RMSE for height to 6.44 cm, with ground measures having higher values with respect to TLS ones. Fig. 9 shows the scatterplots for DBH and height of the 21 trees, as measured by field data collection and TLS.



363  
364  
365  
366  
367  
368  
369  
370  
371

Figure 9. Scatterplots of DBHs (left) and heights (right) for 21 pairs of trees identified in ground and TLS datasets, plotted against the 1:1 line.

Thanks to co-registration of point clouds, the height values for the 21 trees were extracted also from ALS and photogrammetry datasets at 1m spatial resolution; Fig. 10 shows the comparison of heights values from different remotely sensed datasets and the related coefficients of determination ( $R^2$ ).



372  
373  
374  
375  
376  
377  
378  
379  
380  
381  
382  
383  
384  
385  
386

Figure 10. Comparison of heights for 21 trees according to ALS, TLS and photogrammetry measures, with regression line (in red), the 1:1 line (black dashed) and coefficients of determination ( $R^2$ ).

The total above ground biomass (AGB) for the 21 large trees was computed for each dataset using Chave et al. (2005; 2014) allometric equation, using in input the DBHs collected in ground survey, the species-level wood density values, and heights according to the various datasets (Table 3). As from the botanical ground survey, the AGB for the whole 0.7 ha research plot resulted equal to 264.6 Mg, corresponding to 378 Mg ha<sup>-1</sup>. The ratio between the AGB of the 21 trees and that of the whole plot from ground data resulted equal to 0.36. Applying this ratio to other datasets, under the assumption that the differences in height as measured for the pairs by different techniques hold for all the trees in the plot, and thus the error in height measure is similar in tree age classes and species, the amount of AGB per hectare was finally computed per each dataset, as well the differences in tons with respect to ground measured AGB (Table 3).

Table 3. Comparison of AGB values obtained using heights measures from different techniques.

	Ground	TLS	ALS	Photogrammetry
Total AGB for 21 trees (Mg)	95.9	88.6	89.9	91.6

Ratio to ground AGB for 21 trees (%)	100	92.3	93.7	95.5
AGB per hectare	378.0	349.1	354.2	360.8
Difference to ground AGB (264.6 tons)	0	28.9	23.8	17.2

387

#### 388 4. Discussion and conclusions

389 The data collected in the botanical ground survey illustrate that this mature Ghana forest is very diverse in  
390 species composition and highly dense, and the height distribution evidences a multi-layered canopy.  
391 A good agreement between the lidar-derived point cloud and terrestrial lidar and photogrammetric point  
392 clouds was obtained in the co-registration procedure, with mean point distance below 0.5 m in all cases for  
393 the horizontal plane, and below 0.1 m for the vertical plane. The co-registration step is important when  
394 evaluating height as measured from different instruments, as large errors can affect the evaluation.  
395 The DSMs derived from lidar, terrestrial lidar and photogrammetric point clouds evidenced the changes  
396 occurred in the forest in the 4-year period, as in the more recent 2016 datasets (TLS and photogrammetry) a  
397 gap in the canopy was visible, while it was not evident in 2012 ALS data.  
398 The DTMs derived from ALS and TLS appeared very similar, with negligible differences, partly possibly  
399 caused by the difference of four year in datasets acquisition and partly due to the interpolation procedure  
400 applied to ALS data. With photogrammetry data it was not possible to produce a quality DTM due to the  
401 dense canopy cover and thus the poor ground information included in this dataset (Rosca et al., 2018). A  
402 limit to the use of this technique for deriving tree individual metrics is thus represented by the availability of  
403 a high resolution DTM, that should be available or collected from other sources. Birdal et al. (2017) obtained  
404 individual tree heights from a coniferous urban open forest using UAV-based imager, generating the CHM  
405 entirely from photogrammetry data with a 94% correlation and a root-mean-square error of 28 cm with  
406 respect to ground data. However, the authors remarked that this approach is suitable only in open forest.  
407 Further, the co-registration of the PPC with the other datasets relied on feature matching. This means that  
408 either a CHM should be available for (at least part of) the study area, or the absolute positioning of the PPC  
409 should be improved when no reference CHM is available. The UAV used in this study carried a simple GPS  
410 system, resulting in a possible offset of 2-5 m. This can be improved using an RTK-GPS system for the  
411 positioning of the UAV. So when a detailed DTM is present, UAV-based photogrammetry represents a cost-  
412 effective method to frequently detect changes in canopy horizontal structure, but it cannot be operated stand  
413 alone in a tropical forest setting.  
414 On the other hand, with TLS technique accurate DBH information can be obtained in addition to height data:  
415 this represents an advantage when exploring structural changes below the top canopy level, as the DBH  
416 information cannot be captured by ALS or photogrammetric techniques.  
417 The comparison of CHMs at 1 m spatial resolution showed lower maximum and mean height values for  
418 photogrammetry data with respect to the other two datasets. More important, the crown detection with  
419 watershed crown segmentation produced very different results in number of identified trees, with much  
420 lower amount of individuals detected when using photogrammetric data, with respect to ALS and TLS, with  
421 the latter recording the higher number of individuals. Overall the number of detected trees is much less than  
422 what is reported by ground survey, but the difference is reduced when only trees with DBH > 20 cm are  
423 counted. This indicates that ALS and Photogrammetry techniques are not suited for the detection of small  
424 trees, such as the newly recruited ones, a fact also noted using airborne lidar by Dalponte and Coomes  
425 (2016). With TLS those smaller trees can be detected, but this requires a very different approach than  
426 presented here. The mean heights of trees resulted similar among the different datasets, but the histogram of  
427 tree heights from photogrammetric data showed not only less individuals but also a different distribution in  
428 heights compared to the other histograms. At 1 m resolution, the mean trees height resulted slightly higher  
429 with ALS data, followed by TLS and then photogrammetry; at 0.5m the mean heights were generally a bit  
430 lower but comparable for all three techniques. In the result evaluation, the four-year time difference of the  
431 ALS dataset should be considered. In this period, mortality and recruitment of new trees as well as growth  
432 can occur. However, the first two events usually are counterbalanced in old-growth forest leading to minor  
433 changes in tree population, while for large old trees the hydraulic limit reduces the growth in height (Ryan  
434 and Yoder 1997).  
435 These results first indicate that the number of trees that can be detected with the watershed procedure is  
436 much lower than the trees recorded by ground surveys, as expected. However, the number of trees detected

437 from the CHM acquired with ALS and TLS is close to the number of >20 cm DBH trees as recorded in the  
438 ground survey. Ground surveys, either with traditional techniques or TLS remains fundamental for full  
439 inventory purposes. Results from the watershed analysis also indicate that when possible the higher spatial  
440 resolution is not essential, but tree detection parameter settings have to be adapted to suit the right resolution.  
441 For the tree pairs having DBH > 30 cm, a large difference was found between TLS and ground survey  
442 measured heights, almost reaching 2 m. Instead, the agreement between the ALS, TLS and photogrammetric  
443 height for these pairs was very good, with a coefficient of determination around 0.95; this agreement  
444 suggests that overestimation of tree height occurred when collecting data with traditional technique.  
445 Differences in height measurements from field and airborne lidar data were relevant in four Brazilian  
446 Amazon sites, especially for larger trees: ground based measurements of height exceeded airborne lidar  
447 measurements of height by an average of 1.4 m, possibly due to a combination of overestimation by field  
448 measures and underestimation by lidar (Hunter et al. 2013). Instead, a comparison of field vs. lidar measured  
449 height for two commercially significant species in western North America, the Douglas-fir (*Pseudotsuga*  
450 *menziesii*) and the ponderosa pine (*Pinus ponderosa*) evidenced that the field conventional measured were  
451 more accurate than the lidar ones, with the latter also depending on laser beam size (Andersen et al. 2006).  
452 In a United States Pacific Northwest forest, ground survey height data were compared to lidar height data  
453 from leaf-on and leaf-off airborne acquisitions, for > 1000 trees from 45 plots. Overall, lidar error resulted  
454 higher than what estimated by other studies, exceeding 10% of tree height for 60% of the trees and 43% of  
455 the plots at leaf-on and 55% of the trees and 38% of the plots at leaf-off, possibly due to suboptimal  
456 performance of standard preprocessing lidar algorithms (Gatziolis et al. 2010). The contrasting findings of  
457 these studies evidence that the accuracy of height estimated in the ground or by ALS largely depends on  
458 specific site conditions, instruments settings, and the ability of the operators; however measuring tree heights  
459 of cone-shaped species can be easier from the ground, as the tree top can be more evident.  
460 Height data derived from photogrammetry, through a stereomodel combined with a digital terrain model  
461 (DTM) obtained by airborne lidar, were compared to field measured height for 202 *Thuja occidentalis*  
462 individuals, revealing a mean negative bias of 0.88m from photogrammetry (St-Onge et al. 2004).  
463 Underestimation of tree height was also reported by a research comparing Canopy Height Models (CHM)  
464 derived from terrestrial laser scanning (TLS) with the one from UAV-borne laser scanning data, collected  
465 over Netherland forested plots, which showed that TLS could not always detect the top of the canopy (Brede  
466 et al. 2017).  
467 When the AGB for the 21 unequivocally matched pairs was computed, using as input same DBHs (from  
468 ground data) but heights from different techniques, differences emerged as the higher height values recorded  
469 in the ground survey lead to higher AGB. The AGB estimated using ground height values was 7.6 %, 6.3 %,  
470 and 4.5 % higher than that estimated using TLS, ALS photogrammetric heights, respectively. If the ratio  
471 between AGB from 21 trees to that of the entire plot was assumed as constant, the biomass computed using  
472 ground heights resulted 10 %, 9 %, and 6.5 % higher than that estimated using TLS, ALS, and  
473 photogrammetric heights, respectively. These values are similar to those found in other studies: Hunter et al.  
474 (2013) evaluated that the impact of height error on AGB estimation in four Brazilian forest sites caused a 5-  
475 6% uncertainty in the overall plot biomass.  
476 Previous research suggests that in dense forests, where sight occlusion problems occur, ground traditional  
477 techniques can lead to overestimation of tree heights, unless the tree tops are clearly visible and  
478 distinguishable, such as in the case of cone-shaped trees or open forests. On the other hand, with ALS, TLS  
479 and photogrammetry techniques underestimation can occur, in variable amount according to local and  
480 instruments conditions (Wang et al. 2019). We found that same effects in our study area. In comparison,  
481 although limited to smaller areas of maximum few hectares, TLS estimates are most promising since they  
482 provide more robust estimations for DBH, height and volume variables compared to ground instruments  
483 (Gonzales et al., 2018), and provide the full reconstruction of forest in 3D, allowing for additional research  
484 and analysis. Furthermore, advantages were obtained integrating ALS and TLS in assessing single tree  
485 attributes (Giannetti et al. 2018).  
486 Forest density and tree tops visibility represent important characteristics to be initially evaluated. When  
487 enough resources are available, the ALS technique may represent an advantage, as it can cover relatively  
488 large areas in a reduced time, and allows the generation of a DEM. Increasing as much as possible the  
489 number of laser pulses per meter can minimize the chance that the tree tops are missed. TLS is more time-  
490 consuming and data acquisition can be almost as expensive as with ALS over larger areas, with the  
491 disadvantage that from the ground the visibility of tree tops can be reduced, but at the advantage of precise  
492 ground information and DBHs collection. In this study the TLS-derived heights were similar to those

493 obtained by ALS; possibly, this technique is preferable when accurate data on growth or stem density are  
494 needed. From photogrammetric data lower heights were obtained in this research, however the economic  
495 convenience of this techniques supports its use when a DEM is available and for repeated canopy  
496 monitoring. A promising new opportunity is provided by low flying drone-based lidar systems with wide  
497 viewing angles that also record point clouds looking side-ways into forests allowing estimations stem  
498 characteristics such as DBH (Brede et al., 2017).

499 In conclusion, different methods to estimate tree height can be adopted, each with pros and cons, with the  
500 selection of the most appropriate method depending on resources and opportunities. As in other studies, the  
501 different measures caused a remarkable variation in the estimated AGB of this tropical forest. Height is  
502 certainly responsible for a part of the uncertainty associated to AGB estimates: more accurate height  
503 measurements can help to reduce the uncertainty in AGB mapping efforts at any scale. Possibly, the  
504 simultaneous use of different methods can help in correctly estimate height uncertainty and reach a  
505 convergent and accurate result.

#### 506 **Acknowledgments**

507 G.V.L and D.P thank the EU H2020 Grant Agreement No. 640176 (BACI project) for providing partial  
508 support.

#### 509 **References**

510  
511  
512  
513 Andersen, H. E., Reutebuch, S. E., & McGaughey, R. J. (2006). A rigorous assessment of tree height  
514 measurements obtained using airborne lidar and conventional field methods. *Canadian Journal of Remote*  
515 *Sensing*, 32(5), 355-366.

516  
517 Avitabile, V., Herold, M., Heuvelink, G. B., Lewis, S. L., Phillips, O. L., Asner, G. P., ... & Berry, N. J.  
518 (2016). An integrated pan tropical biomass map using multiple reference datasets. *Global change biology*,  
519 22(4), 1406-1420.

520  
521 Banin, L., Feldpausch, T.R., Phillips, O.L., Baker, T.R., Lloyd, J., Affum-Baffoe, K. et al. (2012) What  
522 controls tropical forest achitecture? testing environmental, structural and floristic drivers. *Global Ecology*  
523 *and Biogeography*, 21, 1179–1190.

524  
525 Besl, P. J., & McKay, N. D. (1992, April). Method for registration of 3-D shapes. In *Sensor Fusion IV:*  
526 *Control Paradigms and Data Structures* (Vol. 1611, pp. 586-607). International Society for Optics and  
527 Photonics.

528  
529 Birdal, A. C., Avdan, U., & Türk, T. (2017). Estimating tree heights with images from an unmanned aerial  
530 vehicle. *Geomatics, Natural Hazards and Risk*, 8(2), 1144-1156.

531  
532 Brede, B., Lau, A., Bartholomeus, H. M., & Kooistra, L. (2017). Comparing RIEGL RiCOPTER UAV  
533 LiDAR derived canopy height and DBH with terrestrial LiDAR. *Sensors*, 17(10), 2371.

534  
535 Chave, J., Andalo, C., Brown, S., Cairns, M. A., Chambers, J. Q., Eamus, D., ... & Lescure, J. P. (2005). Tree  
536 allometry and improved estimation of carbon stocks and balance in tropical forests. *Oecologia*, 145(1), 87-  
537 99.

538  
539 Chave, J., Coomes, D., Jansen, S., Lewis, S. L., Swenson, N. G., & Zanne, A. E. (2009). Towards a  
540 worldwide wood economics spectrum. *Ecology letters*, 12(4), 351-366.

541  
542 Chave, J., Réjou  
543 (2014). Improved allometric models to estimate the aboveground biomass of tropical trees. *Global change*  
544 *biology*, 20(10), 3177-3190.

545  
546 Chen, Y., & Medioni, G. (1992). Object modelling by registration of multiple range images. *Image and*  
547 *vision computing*, 10(3), 145-155.

548

-M échain, M

549 Clark, M. L., Clark, D. B., & Roberts, D. A. (2004). Small-footprint lidar estimation of sub-canopy elevation  
550 and tree height in a tropical rain forest landscape. *Remote Sensing of Environment*, 91(1), 68-89.  
551

552 Dalponte, M., & Coomes, D. A. (2016). Tree-centric mapping of forest carbon density from airborne laser  
553 scanning and hyperspectral data. *Methods in ecology and evolution*, 7(10), 1236-1245.  
554

555 Damnyag, L., Saastamoinen, O., Blay, D., Dwomoh, F. K., Anglaaere, L. C., & Pappinen, A. (2013).  
556 Sustaining protected areas: Identifying and controlling deforestation and forest degradation drivers in the  
557 Ankasa Conservation Area, Ghana. *Biological conservation*, 165, 86-94.  
558

559 Edson, C., & Wing, M. G. (2011). Airborne light detection and ranging (LiDAR) for individual tree stem  
560 location, height, and biomass measurements. *Remote Sensing*, 3(11), 2494-2528.  
561

562 Feldpausch, T. R., Lloyd, J., Lewis, S. L., Brienen, R. J., Gloor, M., Monteagudo Mendoza, A., ... &  
563 Alexiades, M. (2012). Tree height integrated into pantropical forest biomass estimates. *Biogeosciences*,  
564 3381-3403.  
565

566 Fowler, A., & Kadatskiy, V. (2011, May). Accuracy and error assessment of terrestrial, mobile and airborne  
567 lidar. In *Proceedings of American Society of Photogrammetry and Remote Sensing Conference (ASPRP*  
568 *2011), Milwaukee, WI, USA* (Vol. 15).  
569

570 Gatzliolis, D., Fried, J. S., & Monleon, V. S. (2010). Challenges to estimating tree height via LiDAR in  
571 closed-canopy forests: a parable from western Oregon. *Forest Science*, 56(2), 139-155.  
572

573 Giannetti, F., Puletti, N., Quatrini, V., Travaglini, D., Bottalico, F., Corona, P., & Chirici, G. (2018).  
574 Integrating terrestrial and airborne laser scanning for the assessment of single-tree attributes in  
575 Mediterranean forest stands. *European Journal of Remote Sensing*, 51(1), 795-807.  
576

577 Gonzalez De Tanago, Jose ; Lau, Alvaro ; Bartholomeus, Harm ; Herold, Martin ; Avitabile, Valerio ;  
578 Raumonon, Pasi ; Martius, Christopher ; Goodman, Rosa C. ; Disney, Mathias ; Manuri, Solichin ; Burt,  
579 Andrew ; Calders, Kim (2018). Estimation of above-ground biomass of large tropical trees with terrestrial  
580 LiDAR, *Methods in Ecology and Evolution* 9 (2). - p. 223 - 234.  
581

582 Goodwin, N. R., Coops, N. C., & Culvenor, D. S. (2006). Assessment of forest structure with airborne  
583 LiDAR and the effects of platform altitude. *Remote Sensing of Environment*, 103(2), 140-152.  
584

585 Hall, J. B., & Swaine, M. D. (1981). Distribution and ecology of vascular plants in a tropical  
586 rain forest: forest vegetation in Ghana. Hague.  
587

588 Hunter, M. O., Keller, M., Victoria, D., & Morton, D. C. (2013). Tree height and tropical forest biomass  
589 estimation. *Biogeosciences*, 10(12), 8385-8399.  
590

591 Kruger, L. M., Midgley, J. J., & Cowling, R. M. (1997). Resprouters vs reseeders in South African forest  
592 trees; a model based on forest canopy height. *Functional Ecology*, 11(1), 101-105.  
593

594 Kwak, D. A., Lee, W. K., Lee, J. H., Biging, G. S., & Gong, P. (2007). Detection of individual trees and  
595 estimation of tree height using LiDAR data. *Journal of Forest Research*, 12(6), 425-434.  
596

597 Larjavaara, M., & Muller-Landau, H. C. (2013). Measuring tree height: a quantitative comparison of two  
598 common field methods in a moist tropical forest. *Methods in Ecology and Evolution*, 4(9), 793-801.  
599

600 Liang, X., Kankare, V., Hyypä, J., Wang, Y., Kukko, A., Haggrén, H., ... & Holopainen, M. (2016).  
601 Terrestrial laser scanning in forest inventories. *ISPRS Journal of Photogrammetry and Remote Sensing*, 115,  
602 63-77.  
603

604 Liu, L.; Pang, Y.; Li, Z. Individual Tree DBH and Height Estimation Using Terrestrial Laser Scanning (TLS)  
605 in a Subtropical Forest. *Sci. Silvae Sin.* 2016, 52, 26–37.  
606

607 Meyer, F., & Beucher, S. (1990). Morphological segmentation. *Journal of visual communication and image*  
608 *representation*, 1(1), 21-46.

609 Molto, Q., Hérault, B., Boreux, J. J., Daullet, M., Rousteau, A., & Rossi, V. (2013). Predicting tree heights  
610 for biomass estimates in tropical forests. *Biogeosciences Discussions*, 10(5), 8611-8635.  
611

612 Plowright A. (2018). ForestTools: Analyzing Remotely Sensed Forest Data. R package version 0.2.0.  
613 <https://CRAN.R-project.org/package=ForestTools>  
614

615 Popescu, S. C., & Wynne, R. H. (2004). Seeing the trees in the forest. *Photogrammetric Engineering &*  
616 *Remote Sensing*, 70 (5), 589-604.  
617

618 Rennie, J. C. (1979). Comparison of height-measurement techniques in a dense loblolly pine plantation.  
619 *Southern Journal of Applied Forestry*, 3(4), 146-148.  
620

621 Roşca, Sabina ; Suomalainen, Juha ; Bartholomeus, Harm ; Herold, Martin (2018). Comparing terrestrial  
622 laser scanning and unmanned aerial vehicle structure from motion to assess top of canopy structure in  
623 tropical forests, *Interface Focus* 8 (2).  
624

625 Ryan, M. G., & Yoder, B. J. (1997). Hydraulic limits to tree height and tree growth. *Bioscience*, 47(4), 235-  
626 242.  
627

628 Saatchi, S. S., Harris, N. L., Brown, S., Lefsky, M., Mitchard, E. T., Salas, W., ... & Petrova, S. (2011).  
629 Benchmark map of forest carbon stocks in tropical regions across three continents. *Proceedings of the*  
630 *National Academy of Sciences*, 108(24), 9899-9904.  
631

632 Srinivasan, S., Popescu, S. C., Eriksson, M., Sheridan, R. D., & Ku, N. W. (2015). Terrestrial laser scanning  
633 as an effective tool to retrieve tree level height, crown width, and stem diameter. *Remote Sensing*, 7(2),  
634 1877-1896.  
635

636 St-Onge, B., Jumelet, J., Cobello, M., & Véga, C. (2004). Measuring individual tree height using a  
637 combination of stereophotogrammetry and lidar. *Canadian Journal of Forest Research*, 34(10), 2122-2130.  
638

639 Theiler, P. W., Wegner, J. D., & Schindler, K. (2013). Markerless point cloud registration with keypoint-  
640 based 4-points congruent sets. *ISPRS Annals of Photogrammetry, Remote Sensing and Spatial Information*  
641 *Sciences*, 1(2), 283-288.  
642

643 Vaglio Laurin, G., Hawthorne, W. D., Chiti, T., Di Paola, A., Gatti, R. C., Marconi, S., ... & Valentini, R.  
644 (2016a). Does degradation from selective logging and illegal activities differently impact forest resources? A  
645 case study in Ghana. *IFOREST-BIOGEOSCIENCES AND FORESTRY*, 9, 354-362.  
646

647 Vaglio Laurin, G., Puletti, N., Hawthorne, W., Liesenberg, V., Corona, P., Papale, D., ... & Valentini, R.  
648 (2016b). Discrimination of tropical forest types, dominant species, and mapping of functional guilds by  
649 hyperspectral and simulated multispectral Sentinel-2 data. *Remote Sensing of Environment*, 176, 163-176.  
650

651 Wallace L, Musk R, Lucieer A. 2014. An assessment of the repeatability of automatic forest inventory  
652 metrics derived from UAV-borne laser scanning data. *IEEE Trans Geosci Remote Sens.* 52:7160–7169.  
653

654 Wang, Y., Lehtomäki, M., Liang, X., Pyörälä, J., Kukko, A., Jaakkola, A., ... & Hyypä, J. (2019). Is field-  
655 measured tree height as reliable as believed—A comparison study of tree height estimates from field  
656 measurement, airborne laser scanning and terrestrial laser scanning in a boreal forest. *ISPRS Journal of*  
657 *Photogrammetry and Remote Sensing*, 147, 132-145.



658

659 Yu, X., Hyypä, J., Hyypä, H., & Maltamo, M. (2004). Effects of flight altitude on tree height estimation  
660 using airborne laser scanning. *Proceedings of the Laser Scanners for Forest and Landscape Assessment–*  
661 *Instruments, Processing Methods and Applications*, 02-06.

662

663 Zarco-Tejada PJ, Diaz-Varela R, Angileri V, Loudjani P. 2014. Tree height quantification using very high  
664 resolution imagery acquired from an unmanned aerial vehicle (UAV) and automatic 3D photo-reconstruction  
665 methods. *Eur J Agron.* 55:89–99.

666

667